Optical excitations of defects in realistic nanoscale silica clusters: Comparing the performance of density functional theory using hybrid functionals with correlated wavefunction methods

M. A. Zwijnenburg,[1,2] C. Sousa,[2] A. A. Sokol,[1] and S. T. Bromley[2,3,a)]
[1]*The Davy Faraday Research Laboratory, The Royal Institution of Great Britain, 21 Albemarle Street, W1S 4BS London, United Kingdom*
[2]*Departament de Química Física and Institut de Recerca de Química Teòrica i Computacional, Universitat de Barcelona, E-08028 Barcelona, Spain*
[3]*Institució Catalana de Recerca i Estudis Avançats (ICREA), 08010 Barcelona, Spain*

(Received 21 February 2008; accepted 19 May 2008; published online 3 July 2008)

Optical excitations of low energy silica $(SiO_2)_4$ clusters obtained by global optimization, as opposed to constructed by hand, are studied using a range of theoretical methods. By focusing on the lowest energy silica clusters we hope to capture at least some of the characteristic ways by which the dry surfaces of silica nanosystems preferentially terminate. Employing the six lowest energy $(SiO_2)_4$ cluster isomers, we show that they exhibit a surprisingly wide range of geometries, defects, and associated optical excitations. Some of the clusters show excitations localized on isolated defects, which are known from previous studies using hydrogen-terminated versions of the defect in question. Other clusters, however, exhibit novel charge-transfer excitations in which an electron transfers between two spatially separated defects. In these cases, because of the inherent proximity of the constituent defects due to the small cluster dimensions, the excitation spectrum is found to be very different from that of the same defects in isolation. Excitation spectra of all clusters were calculated using time-dependent density functional theory (TD-DFT) and delta-SCF DFT (ΔDFT) methods employing two different hybrid density functionals (B3LYP and BB1K) differing essentially in the amount of incorporated Hartree–Fock-like exchange (HFLE). In all cases the results were compared with CASPT2 calculated values which are taken as a benchmark standard. In line with previous work, the spatially localized excitations are found to be well described by TD-DFT/B3LYP but which gives excitation energies that are significantly underestimated in the case of the charge-transfer excitations. The TD-DFT/BB1K combination in contrast is found to give generally good excitation energies for the lowest excited states of both localized and charge-transfer excitations. Finally, our calculations suggest that the increased quality of the predicted excitation spectra by adding larger amounts of HFLE is mainly due to an increased localization of the excited state associated with the elimination of spurious self-interaction inherent to (semi-)local DFT functionals. © *2008 American Institute of Physics*. [DOI: 10.1063/1.2943147]

INTRODUCTION

Silica (SiO_2) nanostructures, synthesized in a variety of morphologies (e.g., mesoporous materials, nanotubes, nanoparticles), have attracted much recent attention due to their interesting optical properties, most notably room temperature red,[1–4] green,[3–5] blue,[3,5–8] and white[9] photoluminescence (PL). Bulk silica is wide-gap material with the conduction states positioned close to the vacuum zero energy with valence states well localized on the oxygen sublattice. In this situation the model of quantum confinement,[10] often invoked to explain the PL properties of nanoscale silicon, does not seem to explain the observed phenomena in nanosilica. However, as all forms of nanosilica have inherently high surface areas, it's tempting to relate the observed PL to the presence of specific defects terminating the material's surface. Recently, some of us have studied the low energy landscape of small silica clusters [$(SiO_2)_N$ with $5<N<28$] by means of global optimization techniques.[11,12] Due to their small size these clusters have a large proportion of atoms at terminating or "surface" sites and are thus natural model systems of the dry surfaces of nanosilica.[13,14] We regard such an approach for obtaining defective cluster systems as more objective than constructing model clusters as it avoids bias associated with the choice of defect and the immediate environment in which it resides. In these studies it was observed that low energy silica clusters are characterized by a diverse range of different structural motifs and terminating defects. The latter is defined as any structural motif different from corner-sharing SiO_4 tetrahedra (i.e., four-coordinated silicon atoms linked by two-coordinated oxygen atoms) as found in the bulk. Examples of such defects are the silanone group (=Si=O) and the Si_2O_2 two-membered ring.

In order to understand the optical properties of these defects, and how they are affected by the type of cluster they terminate, it is necessary to have access to both the electronic ground state and the lowest lying electronic excitations of the

a)Electronic mail: stefan.bromley@icrea.cat.

combined cluster-defect system. In experiments, although one can obtain the optical absorption and PL spectra, due to current limits of characterization it is impossible to unambiguously assign a structural defect to such data without the input from accurate calculations. While for the ground state one can use density functional theory (DFT), which has been successfully applied to a range of similar silica systems,[11,12,15–19] the calculation of electronic excitations often requires more elaborate treatments. Correlated wave function methods, such as configuration interaction (CI) and coupled cluster (CC) theory, have been applied in this context,[20–24] but the usage of such methods for only but the smallest clusters quickly becomes computationally prohibitive as the size of the calculation scales with the number of electrons in the cluster to the power of six or more. Time-dependent DFT (TD-DFT),[25,26] for which the computational expense scales much more conveniently with the size of the problem at hand, is an appealing alternative as it allows one to study a much wider size-range of system. The quality of the calculated excited states, however, is as always with DFT, strongly dependent on the ability of the chosen density functional to correctly reproduce the relevant physics.

In one of the first applications of TD-DFT to silica, Raghavachari and co-workers[27] showed that the method, in combination with the B3LYP (Ref. 28) hybrid density functional, gives results that are within a couple tenths of an eV of the experimental or correlated wave function values for the lowest excitations of a range of silica defects (represented as small molecular clusters terminated with hydroxyl groups). The TD-DFT/B3LYP approach has subsequently become the functional of choice to study the optical properties of silica. Recent work by To *et al.*[29] and Kimmel *et al.*,[30] however, shows that TD-DFT/B3LYP fails to provide reliable excitation energies of the neutral aluminium defect in α-quartz. They further show that the application of the BB1K (Becke88-Becke95 one-parameter model for kinetics[31]) or a modified B3LYP (Ref. 30) hybrid functional, incorporating a higher fraction of Hartree–Fock-like exchange (HFLE), 42%, respectively, 32.5% as opposed to 20% in the B3LYP functional, leads to considerably more accurate results with respect to experiment. The problem that TD-DFT/B3LYP has in reproducing the excitations for this defect most likely lies in the poor description of the ground state rather than the excited states.[29,30,32–36] B3LYP, due to spurious self-interaction, smears the unpaired electron out over all four oxygen atoms around the aluminium centre. In contrast, BB1K (and other hybrid functionals with more HFLE than B3LYP) recover the experimental result that finds the electron to be localized on only one of the four oxygen atoms. Hybrid functionals with relatively increased proportions of HFLE in TD-DFT calculations have also been successfully applied to the excited states of organic molecules,[37,38] for which the excited state and not the ground state is poorly described. These combined findings raise the question of whether using functionals with more HFLE than B3LYP is also beneficial for more accurate TD-DFT descriptions of excited states in nanoscale silica and related inorganic materials for which the ground state is accurately described by B3LYP. To help shed light on this issue we have calculated the optical excitations of six of the lowest energy cluster isomers of Si_4O_8, using both TD-DFT/B3LYP and TD-DFT/BB1K, and compared the results obtained with benchmark values from correlated wavefunction-based complete active space second-order perturbation theory[39,40] (CASPT2) calculations. The low energy isomer spectrum of Si_4O_8 clusters is found to exhibit a surprisingly rich variety of structural motifs while still small enough to be efficiently treated with CASPT2, thus allowing us to evaluate the performance of both flavors of TD-DFT for a realistic diversity of defects.

COMPUTATIONAL DETAILS

In order to obtain the low energy isomer spectrum of Si_4O_8 clusters, following previous studies,[11,12] we combined the use of an interatomic potential, specifically developed for the study of nanosilica,[41] with the basin-hopping global optimization algorithm.[42] Subsequently all clusters resulting from this procedure (approximately 15 distinct clusters) were optimized with respect to their energies and structures using DFT calculations, employing either the B3LYP (Ref. 28) or BB1K (Ref. 31) hybrid functionals, as implemented in the GAUSSIAN03 code.[43] A 6-31G* Pople basis set[44,45] was used in the optimizations for all atoms, which includes a single polarization function on each atom, i.e., a $[4s\ 3p\ 1d]$ contracted basis for Si and $[3s\ 2p\ 1d]$ for O. All usage of symmetry in the calculations was explicitly disabled, and for the numerical integration, an ultrafine grid (a pruned grid with 99 radial shells and 590 angular points per shell) was employed. The total energies of all clusters were finally evaluated employing the optimized B3LYP/6-31G* geometries and the Dunning augmented correlation consistent polarized valence triple-zeta (aug-cc-pVTZ) basis set[46,47] including diffuse and polarization functions on every atom (i.e., a $[6s\ 5p\ 3d\ 2f]$ contracted basis for Si and $[5s\ 4p\ 3d\ 2f]$ for O). It is noted that the cluster energies of this procedure are negligibly different (<0.004 eV/SiO_2 total energy) to the cluster energies after full optimizations using B3LYP/aug-cc-pVTZ. Although not so important for very small clusters, this general procedure provides a reliable and computationally more efficient means for obtaining accurate optimized cluster energies which can be reasonably employed for larger silica systems. The six lowest energy clusters obtained from this procedure (all lying within an energy range 0.65 eV/SiO_2; see Fig. 1) were used in the calculations of the excited states.

The lowest lying excited states of all clusters were calculated using the linear-response version of TD-DFT,[48–50] and for the lowest triplet excited state, also by ΔDFT. In the latter case the excitation energy is calculated as the difference in DFT energy of the lowest triplet state (obtained through constrained SCF and subsequently verified by stability analysis[51,52]) and the singlet ground state of a cluster. All further computational details are similar to those used for the ground state geometry optimizations with the exception that, for some calculations, the aug-cc-pVTZ basis was used. The application of the latter allowed us to probe the influence of the size of the basis set on the TD-DFT results obtained.

The ground and low-lying excited states of the selected

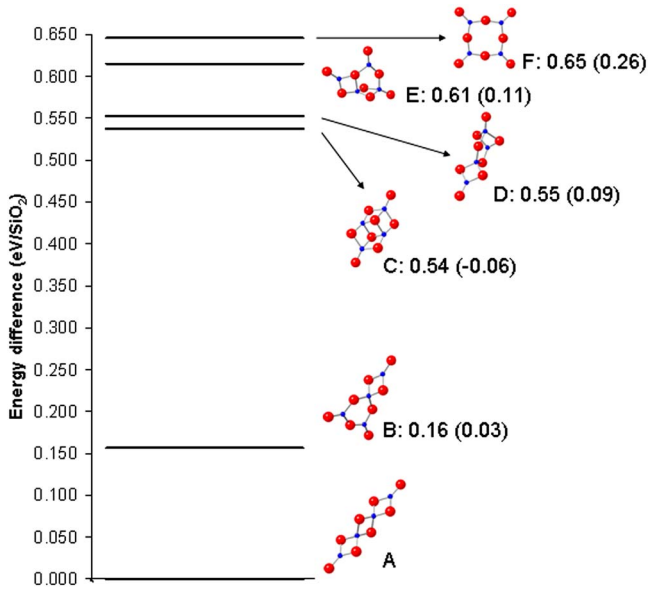

FIG. 1. (Color online) Relative total energies (eV/SiO_2) of the six lowest energy Si_4O_8 cluster isomers evaluated employing the optimised B3LYP/6-31G* geometries and B3LYP with the Dunning augmented correlation consistent polarized valence triple-zeta (aug-cc-pVTZ) basis. The values in parentheses denote the differences with resepect to the corresponding relative energies obtained using CASPT2 (E_{rel}[CASPT2]−E_{rel}[DFT]). Large red spheres denote oxygen centers and small blue spheres silicon centers.

Si_4O_8 clusters were also calculated using the complete active space second-order perturbation theory[39,40] (CASPT2) method, as implemented in the MOLCAS-6 package.[53] In this approach, first an *N*-electron CASSCF wavefunction is computed, which includes an important part of the electron correlation effects in a variational way, and in a second step, the remainder, mainly dynamical electron correlation, is obtained by a second-order perturbational treatment with the CASSCF wave function as zeroth-order wavefunction. This strategy has been successfully applied to study excited states in solid-state compounds[54–56] including the study of the optical spectra of point defects in silica.[57] In the CASPT2 calculations the augmented correlation consistent polarized valence double-zeta basis (aug-cc-pVDZ) (Refs. 46 and 47) (i.e., a [5*s* 4*p* 2*d*] contracted basis for Si and [4*s* 3*p* 2*d*] for O) was used for the wavefunction for all atoms. This choice was found in the excitation energies of less than 0.2 eV with respect to a larger modified aug-cc-pVTZ benchmark basis (i.e., a [6*s* 5*p* 3*d* 2*f*] contracted basis for Si and [5*s* 4*p* 3*d* 2*f*] for O). The CASSCF wavefunctions were constructed according to the point symmetry group of the systems. To define the active space, restricted active space SCF (RASSCF) calculations have been performed and the orbitals with the largest deviation from 0 or 2 in the natural orbital occupation numbers were included in the active space. Thus, the final active space includes either 12 orbitals and 12 electrons (cluster A, C, and D), 14 orbitals and 14 electrons (cluster B and E) or 16 orbitals and 16 electrons (cluster F). All valence electrons (Si-3*s*, 3*p* and O-2*s*, 2*p*) were correlated in the CASPT2 calculations.

RESULTS AND DISCUSSION

Table I gives the lowest allowed singlet excitations for the six clusters studied, as obtained with TD-DFT/B3LYP, TD-DFT/BB1K, and CASPT2. The CASPT2 excitations calculated using either B3LYP or BB1K DFT-optimized cluster geometries were found to be similar and the latter values are taken for most comparisons hereafter. The CASPT2 values calculated using the BB1K optimized cluster geometries span the range of 3.19–5.67 eV, where the clusters terminated with silanone groups (A, B, F) are found to start absorbing light at higher photon energies (5.27–5.67 eV) than the clusters terminated by other defects (3.19–5.07 eV). Taking into account differences in local geometry the former value fits rather well with multireference double-excited CI (MRCI) and CC values of 5.7–5.73 eV obtained for an isolated silanone defect (modeled by a hydrogen-terminated $(H_3SiO)_2Si{=}O$ fragment) by Raghavachari and Pacchioni.[24]

Table II gives the lowest triplet excitation energies for the BB1K optimized geometries of the six clusters studied, as obtained with TD-DFT/B3LYP, TD-DFT/ BB1K, ΔDFT/B3LYP, ΔDFT/BB1K, and CASPT2. The lowest triplet excitations are found to lie below the lowest singlet excitations by 0.1–0.6 eV and for the rest behave similarly to the lowest allowed singlet excitation values discussed above. More interestingly, the variational ΔDFT and linear-response TD-DFT calculations of the lowest triplet excitation energies generally give very similar results.

An analysis of the highest occupied molecular orbital (HOMO) and lowest unoccupied molecular orbital (LUMO)

TABLE I. Vertical excitation energies (in eV) for the lowest allowed optical excitations of clusters A–F computed using different computational approaches and geometries optimized at the DFT level (BB1K, B3LYP functionals). Values between parentheses are obtained with a aug-cc-pVTZ basis-set instead of the standard 6-31G* (DFT)/aug-cc-pVDZ (CASPT2) basis set for all other values.

	BB1K geometry			B3LYP geometry		
Cluster	TD-DFT BB1K	TD-DFT B3LYP	CASPT2	TD-DFT BB1K	TD-DFT B3LYP	CASPT2
A	5.75(5.70)	5.26(5.16)	5.67	5.57(5.54)	5.10(5.06)	5.51(5.29)
B	5.59	4.94	5.54	5.40	4.77	5.25
C	4.40(4.50)	3.37(3.46)	4.41	4.29(4.39)	3.28(3.37)	4.23(4.10)
D	3.09(3.18)	2.04(2.12)	3.19	2.70(2.80)	1.70(1.78)	2.86
E	4.47	3.12	5.07	4.32	2.98	5.07
F	5.56	4.85	5.27	5.37	4.68	5.08

TABLE II. Vertical excitation energies (in eV) for the lowest triplet excitations of clusters A–F computed using different computational approaches and geometries optimized using the BB1K functional. Values between parentheses are obtained with a aug-cc-pVTZ basis-set instead of the standard 6-31G* (DFT)/aug-cc-pVDZ (CASPT2) basis-set for all other values.

Cluster	TD-DFT BB1K	TD-DFT B3LYP	ΔDFT BB1K	ΔDFT B3LYP	CASPT2
A	5.23(5.23)	4.80(4.80)	5.11	5.11	5.37
B	5.18	4.62	5.08	4.93	5.05
C	4.19(4.29)	3.21(3.30)	4.27	3.59	4.33
D	2.97(3.07)	1.94(2.03)	3.09	2.86	3.19
E	4.37	3.05	4.62	⋯	5.18
F	4.99	4.33	4.96	4.57	5.53

of the electronic ground state together with population analysis on the excited state density from the ΔDFT and CASSCF calculations suggests that the studied clusters show two fundamentally different types of excitations. For the clusters terminated with silanone groups (A, B, F), the excitation is found to take place predominantly on the terminal silanone groups and involves the excitation of an electron from an nonbonding oxygen $2p$ orbital to an antibonding σ^* orbital (see Fig. 2). Clusters C and D are not only terminated by silanone groups but also contain triply and singly coordinated oxygen atoms (≡Si−O). Note, the latter oxygen termination is not the well-known open-shell non-bridging oxygen hole centre (≡Si−O·), with our DFT calculations giving a closed-shell ground state for cluster C with all $2p$ orbitals on the singly coordinated oxygen completely filled and with the remaining hole located on the silicon atoms around the two three-coordinated oxygen atoms.[11] Effectively, the singly coordinated oxygen is thus negatively charged while the silicon atoms around the triply coordinated oxygen gain positive charge. Recently, the nonbridging oxygen hole center has been shown to be an efficient electron trap[58] giving rise to a closed-shell terminating oxygen defect analogous to our defect. The difference in our case is that the closed-shell oxygen terminations are internally charge compensated by the triply coordinated oxygen atoms in the cluster (i.e., not from an external source of charge as in Ref. 58). As such, this self-compensating defect pair constitutes a natural low energy surface reconstruction for dry nanosilica[11] surfaces. Upon excitation in such a defect a hole transfers to a singly coordinated oxygen center (or, alternatively, one electron from a $2p$ orbital on the singly coordinated oxygen centre transfers to the atoms around the triply coordinated oxygen center, see Fig. 2). Cluster E, finally, is a variant on clusters C and D in which the hole, instead of being on silicon atoms around a triply coordinated oxygen center in the ground state, resides on a triply coordinated silicon center. A similar defect (a combination of ≡Si−O$^-$ and ≡Si$^+$ centers in close proximity) has recently been proposed by Martinez *et al.*[59] as a possible point defect in thin silica films.

The calculated excitation spectra provide useful insights into the ability of DFT-based methods to describe accurately absorption spectra in a range of realistic oxide clusters exhibiting a variety of surface defects. The root mean square deviations in excitation energy between TD-DFT and CASPT2 (ΔE_{RMS}) for the three lowest singlet excitations are shown in Table III. For some of these clusters (A, B, F), we find, just as for earlier studies,[27] a reasonably good quantitative match ($\Delta E_{RMS} \leqslant 0.61$ eV) between TD-DFT/B3LYP and correlated wavefunction results. For the same three clusters TD-DFT/BB1K calculations are also found to give similar excitation values, which appear to reproduce even slightly better the CASPT2 values ($\Delta E_{RMS} \leqslant 0.23$ eV). For both

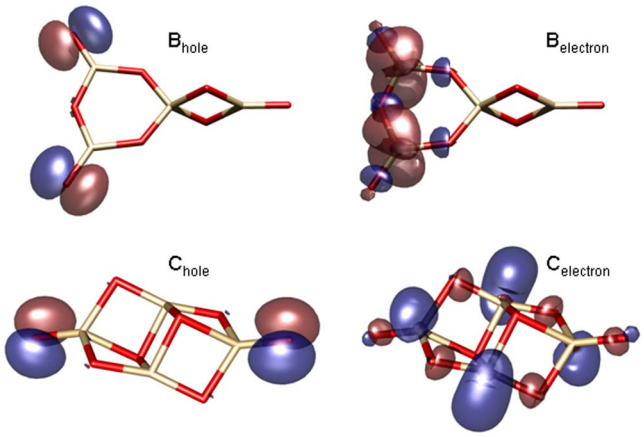

FIG. 2. (Color online) Molecular orbitals (as obtained from an average of all configurations from the relevant energy levels in the CASSCF calculations) corresponding to the transferred electron and remaining hole for the lowest excited state for clusters B and C.

TABLE III. Root mean square difference between the DFT and CASPT2 calculated values for the three lowest singlet excitations of clusters A–E and the four lowest singlet excitations of clusters F. Values between parentheses are obtained with a aug-cc-pVTZ basis-set instead of the standard 6-31G* (DFT)/aug-cc-pVDZ (CASPT2) basis-set for all other values. The entry "Sum" corresponds to the root mean square difference calculated using the excitations of all the clusters combined.

	BB1K geometry		B3LYP geometry	
Cluster	TD-DFT BB1K	TD-DFT B3LYP	TD-DFT BB1K	TD-DFT B3LYP
A	0.09	0.38	0.07(0.26)	0.38(0.18)
B	0.14	0.56	0.18	0.44
C	0.02	1.03	0.06(0.22)	0.95(0.82)
D	0.44	1.01	0.42	0.97
E	0.57	1.78	0.65	1.83
F	0.23	0.61	0.21	0.61
Sum	0.31	0.97	0.36	0.97

B3LYP and BB1K, the corresponding ΔDFT results follow a similar pattern. However, the situation is completely different for clusters C, D, and E where, depending on the cluster in question, the TD-DFT/B3LYP predicted excitation energy values are found to lie 0.7–2 eV below the CASPT2 results. In contrast, TD-DFT/BB1K gives very good quantitative agreement with the benchmark CASPT2 data for clusters C and D ($\Delta E_{\mathrm{RMS}} \leqslant 0.44$ eV). For cluster E, although the agreement with CASPT2 becomes poorer ($\Delta E_{\mathrm{RMS}} \leqslant 0.65$ eV), it should be noted that the disagreement using TD-DFT/B3LYP is significantly worse ($\Delta E_{\mathrm{RMS}} = 1.75-1.85$ eV). We also find a similar trend for the ΔDFT calculations with respect to these clusters, which, however, for B3LYP recovers some of the large discrepancies with respect to the CASPT2 results for cluster D.

The effect of increasing the basis set beyond 6-31G* with diffuse functions on the excitation energies in Tables I and II and the RMS differences in Table III is found to be small (typically less than 0.1 eV) for all clusters where it was considered. This is perhaps not surprising as all of the excitations are localized and show no Rydberg character (see above). The effect of geometry on the calculated excitation is also found to be small and consistent. For all methods (TD-DFT/BB1K, TD-DFT/B3LYP, and CASPT2), the excitations for the B3LYP optimized geometry are of the order of 0.2 eV lower than for the structures optimized with the BB1K functional. This constant shift in excitation energies between both geometries is most likely the direct result of the fact that all bond lengths in the B3LYP optimized structure are ~0.02 Å longer than those in the BB1K optimized geometries.

The calculation of excitation energies involves taking the difference between the energies of the ground state and the lowest lying excited states. As discussed in the Introduction, other studies on siliceous systems have noted that problems in describing correctly excitation energies can originate in a poor description of the electronic ground state by DFT. In order to confirm that the electronic ground states of the six studied clusters were well described by DFT, we compared their relative total energies and electron densities as obtained from B3LYP and CASPT2 using a triple-zeta basis. In both sets of calculations the same B3LYP optimized geometries were employed. The correspondence between the two sets of energies was found to be typically good (differences less than 0.11 eV; see Fig. 1) with the same energetic ordering of all cluster isomers reproduced by both methods. Only for highest energy isomer (cluster F) was a larger difference found between the calculated ground state relative energies. We note that, even in this case, the electronic densities in the two calculations were very similar suggesting that the electronic character of the ground state is still comparable.

Having ascertained that the electronic ground states of our clusters are generally well described by hybrid DFT in the remainder we focus on excited states. In clusters A, B, and F the electron excitation is centred around single sites; the terminal silanone groups. In contrast, as noted above, excitations within clusters C, D, and E involve transfer of excited electrons between two spatially separated sites and thus imply substantial charge transfer (CT). Furthermore, while the orbitals involved in the excited states of clusters A, B, and F are well localized, the CT excited electron states of clusters C, D, and E show a considerable delocalization over the whole cluster (see examples in figure 2). The description of systems displaying CT behavior and/or (de)localization is known to be problematic for (TD-)DFT.

From previous work on organic systems, it is known that chromophore CT states calculated using pure DFT (i.e., GGA or LDA) underestimate values from experiment and/or correlated wavefunction methods by up to several eV.[37,60–63] Different explanations for this failure of TD-DFT are suggested in the literature[62–65] and it has been noted that using hybrid functionals can (partly) repair this deficiency, although the apparent amount of HFLE required is system dependent and can be much higher than the 20% in TD-DFT/B3LYP (up to 50%).[37,38] Other work on organic molecules has shown that for systems with delocalized states (e.g., conjugated π systems) pure DFT also predicts excitation energies that are significantly lower than those obtained from experiment or correlated wavefunction methods.[66,67] Again the use of hybrid functionals is found to be an improvement over pure DFT. Although the situation for our clusters is not exactly the same as for organic systems (e.g., organic CT excitations are between well-separated (5–15 Å) molecules but in our case both sites involved in the transfer are located in close proximity in the same cluster, <4.5 Å) we observe the same trends for silica clusters. Spatially localized non-CT excitations (clusters A, B, and F) are well described by both TD-DFT/B3LYP and TD-DFT/BB1K while clusters with CT states where the excited electron is considerably delocalized (clusters C, D, and E) require the amount of HFLE in the BB1K functional or even more (cluster E). From our results, it is difficult to assess which deficiency (either delocalization, CT or both) is repaired by the addition of increased proportions of HFLE, and thus we currently regard it as an empirical correction. However, it should be stressed that adding HFLE (at least up to 40%) systematically improves all spectra, the induced shift in energy spectra is not the same for all clusters. The results presented in Fig. 3 show, for example, that the TD-DFT and ΔDFT calculated excitation energies for the lowest triplet excitation in cluster C increase linearly with the amount of added HFLE and furthermore are extremely strongly correlated. This suggests that the underestimation of the excitation energy with TD-DFT and ΔDFT for pure GGA (or low HFLE hybrid functionals) has a similar origin in both methods.

Finally, we note that the exclusively silanone-terminated clusters (A, B, F) show an interesting trend between $(SiO)_n$ n-membered-ring strain and absorption onset. Previous work[68] has demonstrated that the ring size and the associated strain energy in silica decreases strongly in the order two-membered ring > three-membered ring > four-membered ring, where the latter is found to be almost ring-strain free. When moving from an inherently highly strained system (cluster A, where the silicon centre of the silanone group is part of a two-membered ring) to lesser (cluster B with the silicon of the silanone groups forming part of either a two or three-membered ring) and an even lesser strained systems (cluster F where the silicon of the silanone groups forms part of a four-membered ring) the absorption onset consistently

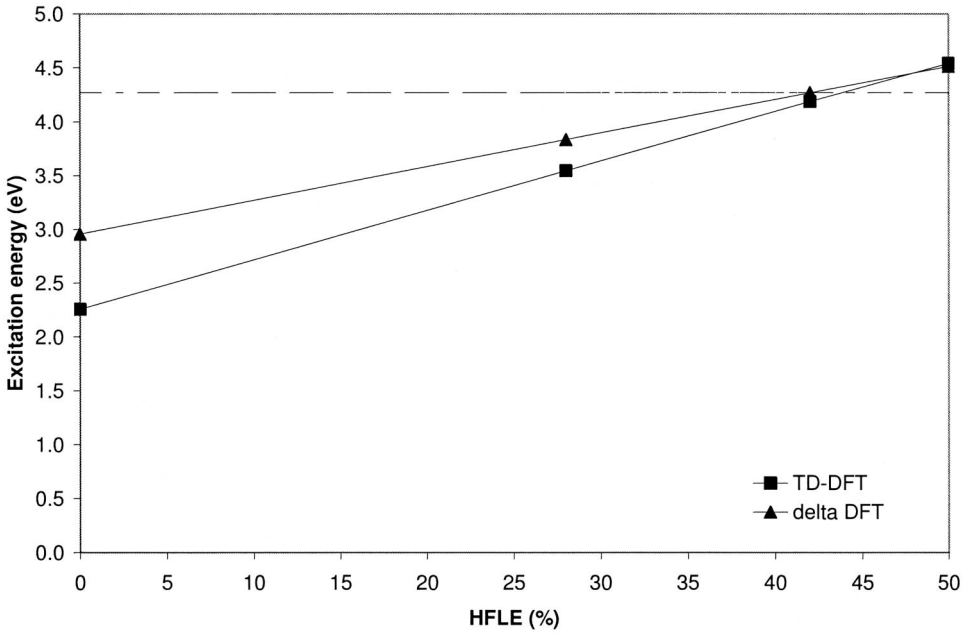

FIG. 3. Change in the TD-DFT and ΔDFT calculated excitation energy from the ground state to the lowest triplet excitation of cluster C (^3B_g) as a function of the amount of HFLE. The dashed line indicates the energy from the CASPT2 calculations.

lowers. This observation is confirmed by the spin populations from ΔDFT and CASSCF calculations on cluster B, which show that the excitations involving the silanone group whose silicon forms part of the two-membered ring lie higher in energy than those involving the silicon centres which form part of the three-membered ring.

CONCLUSIONS

Optical excitations of small low energy silica clusters obtained through global optimization methods are studied using a range of theoretical approaches. The calculations show that there is a surprisingly wide range of possible optical excitations in these clusters and by analogy possibly exhibited on dry silica surfaces. Some of these excitations are found to take place on an isolated defect, while others correspond to an electron transferring between two spatially separated defects and thus have a CT character. The performance of TD-DFT using two different hybrid density functionals, B3LYP and BB1K, differing essentially in the amount of HFLE (20% and 42%, respectively), was compared with CASPT2 calculation as benchmark standard. In line with previous work, the spatially localized excitations are found to be well described by TD-DFT/B3LYP but this methodology gives excitations energies that are considerably too low in the case of the CT excitations. In contrast, the TD-DFT/BB1K combination gives generally good excitation energies for the lowest excited states of both localized and charge-transfer excitations. For one cluster with charge-transfer excitations the quantitative match with CASPT2 was shown to further improve with adding in even a larger amount of HFLE than present in BB1K. In contrast the effect of increasing the basis-set with diffuse basis functions and the choice of DFT functional used to optimize the ground state geometry was found to be small. The large positive effect on the quality of the calculated excitation energies of adding increasing amounts of HFLE is demonstrated to be most likely due to an increased localization of the excited state, as the result of the elimination of spurious self interaction inherent to (semi) local DFT functionals.

By concentrating only on inherently low energy silica nanoclusters, rather than clusters designed by hand, we hope that our study points to a way to capture at least some of the characteristic and realistic ways by which the dry surfaces of silica nanosystems preferentially terminate. Although in this investigation we have employed relatively small clusters and focussed on the reliability of theoretical methods to treat their excitations, in further studies we will build on the knowledge gained to treat larger more realistic systems.

ACKNOWLEDGMENTS

We kindly acknowledge Dr. R. G. Bell, Dr. M. Head-Gordon, Dr. F. Illas, Dr. A. Schluger, and Dr. P. Sushko for stimulating discussion, and Dr. J. C. Wojdel for his assistance with preparing Fig. 2. M.A.Z. acknowledges the European Commission for a Marie Curie Intra-European Fellowship (MEIF-CT-2005-010326) and a HPC-Europa travel grant. This study has further been supported by the Spanish Ministry of Education and Science (Grant No. CTQ2005-08459-CO2-01), by the Generalitat de Catalunya (Grant No. 2005SGR00697) and by the COST-D41 action. Computational time on the computers of the Centre de Supercomputació de Catalunya (CESCA) is gratefully acknowledged.

[1] Yu. D. Glinka, A. S. Zyubin, A. M. Mebel, S. H. Lin, L. P. Hwang, and Y. T. Chen, Eur. Phys. J. D **16**, 279 (2001).
[2] A. S. Zyubin, Yu. D. Glinka, A. M. Mebel, S. H. Lin, L. P. Hwang, and Y. T. Chen, J. Chem. Phys. **116**, 281 (2002).
[3] Yu. D. Glinka, S. H. Lin, and Y. T. Chen, Phys. Rev. B **66**, 035404 (2002).
[4] Y. Yang, B. K. Tay, X. W. Sun, H. M. Fan, and Z. X. Shen, Physica E (Amsterdam) **31**, 218 (2006).
[5] M. Zhang, E. Ciocan, Y. Bando, K. Wada, L. L. Cheng, and P. Pirouz, Appl. Phys. Lett. **80**, 491 (2002).
[6] Yu. D. Glinka, S. H. Lin, and Y. T. Chen, Phys. Rev. B **62**, 4733 (2000).
[7] Y. Hao, G. Meng, C. Ye, and L. Zhang, Appl. Phys. Lett. **87**, 033106 (2005).
[8] A. Aboshi, N. Kurumoto, T. Yamada, and T. Uchino, J. Phys. Chem. C

111, 8483 (2007).
[9] T. Uchino and T. Yamada, Appl. Phys. Lett. **85**, 1164 (2004).
[10] A. D. Yoffe, Adv. Phys. **50**, 1 (2001).
[11] E. Flikkema and S. T. Bromley, J. Phys. Chem. B **108**, 9638 (2004).
[12] S. T. Bromley and E. Flikkema, Phys. Rev. Lett. **95**, 185505 (2005).
[13] L. S. Weng, J. B. Nicholas, M. Dupuis, H. Wu, and S. D. Colson, Phys. Rev. Lett. **78**, 4450 (1997).
[14] S. T. Bromley, M. A. Zwijnenburg, and Th. Maschmeyer, Surf. Sci. **539**, L554 (2003).
[15] R. Q. Zhang, T. S. Chu, and S. T. Lee, Chem. Phys. **114**, 5531 (2001).
[16] S. T. Bromley, M. A. Zwijnenburg, and Th. Maschmeyer, Phys. Rev. Lett. **90**, 035502 (2003).
[17] M. A. Zwijnenburg, S. T. Bromley, E. Flikkema, and Th. Mashmeyer, Chem. Phys. Lett. **385**, 389 (2004).
[18] M. W. Zhao, R. Q. Zhang, and S. T. Lee, Phys. Rev. B **69**, 153403 (2004).
[19] P. V. Avramov, I. Adamovic, K. M. Ho, C. Z. Wang, W. C. Lu, and M. S. Gordon, J. Phys. Chem. A **109**, 6294 (2005).
[20] G. Pacchioni and G. Ierano, Phys. Rev. Lett. **79**, 753 (1997).
[21] G. Pacchioni and G. Ierano, Phys. Rev. B **56**, 7304 (1997).
[22] G. Pacchioni and G. Ierano, Phys. Rev. B **57**, 818 (1998).
[23] G. Pacchioni, G. Ierano, and A. M. Marquez, Phys. Rev. Lett. **81**, 377 (1998).
[24] K. Raghavachari and G. Pacchioni, J. Chem. Phys. **114**, 4657 (2001).
[25] E. Runge and E. K. U. Gross, Phys. Rev. Lett. **52**, 997 (1984).
[26] E. K. U. Gross and K. Burke, Lect. Notes Phys. **706**, 1–17 (2006).
[27] K. Raghavachari, D. Ricci, and G. Pacchioni, J. Chem. Phys. **116**, 825 (2002).
[28] A. D. Becke, J. Chem. Phys. **98**, 5648 (1993).
[29] J. To, A. A. Sokol, S. A. French, N. Kaltsoyannis, and C. R. A. Catlow, J. Chem. Phys. **122**, 144704 (2005).
[30] A. V. Kimmel, P. V. Sushko, and A. L. Schluger, J. Non-Cryst. Solids **353**, 599 (2007).
[31] Y. Zhao, B. J. Lynch, and D. G. Truhlar, J. Phys. Chem. A **108**, 2715 (2004).
[32] X. Solans-Montfort, V. Branchadell, M. Sodupe, M. Sierka, and J. Sauer, J. Chem. Phys. **121**, 6034 (2004).
[33] G. Paccioni, F. Frigoli, D. Ricci, and J. Weil, Phys. Rev. B **63**, 054102 (2000).
[34] J. Laegsgaard and K. Stokbro, Phys. Rev. Lett. **86**, 2834 (2001).
[35] M. Nolan and G. W. Watson, J. Chem. Phys. **125**, 144701 (2006).
[36] S. Sicolo, G. Palma, C. Di Valentin, and G. Pacchioni, Phys. Rev. B **76**, 075121 (2007).
[37] R. J. Maygar and S. Tretiak, J. Chem. Theory Comput. **3**, 976 (2007).
[38] A. Pinter, G. Haberhauer, I. Hyla-Kryspin, and S. Grimme, Chem. Commun., 3711 (2007).
[39] K. Andersson, P. A. Malmqvist, B. O. Roos, A. J. Sadlej, and K. Wolinski, J. Phys. Chem. **94**, 5483 (1990).
[40] K. Andersson, P. A. Malmqvist, and B. O. Roos, J. Phys. Chem. **96**, 1218 (1992).
[41] E. Flikkema and S. T. Bromley, Chem. Phys. Lett. **378**, 622 (2003).
[42] D. J. Wales and J. P. K. Doye, J. Phys. Chem. A **101**, 5111 (1997).
[43] M. J. Frisch, G. W. Trucks, H. B. Schlegel *et al.*, GAUSSIAN 03, revision C.02, Gaussian, Inc., Wallingford, CT, 2004.
[44] P. C. Hariharan and J. A. Pople, Theor. Chim. Acta **28**, 213 (1973).
[45] M. M. Francl, W. J. Petro, W. J. Hehre, J. S. Binkley, M. S. Gordon, D. J. deFrees, and J. A. Pople, J. Chem. Phys. **77**, 3654 (1982).
[46] T. H. Dunning, Jr., J. Chem. Phys. **90**, 1007 (1989).
[47] D. E. Woon and T. H. Dunning, Jr., J. Chem. Phys. **98**, 1358 (1993).
[48] M. E. Casida, in *Recent Advances in Density Functional Methods*, edited by D. P. Chong (World Scientific, Singapore, 1995), Vol. 1.
[49] R. Bauernschmitt and R. Ahlrichs, Chem. Phys. Lett. **256**, 454 (1996).
[50] R. E. Stratmann, G. E. Scuseria, and M. J. Frisch, J. Chem. Phys. **109**, 8218 (1998).
[51] R. Seeger and J. A. Pople, J. Chem. Phys. **66**, 3045 (1977).
[52] R. Bauernschmitt and R. Ahlrichs, J. Chem. Phys. **104**, 9047 (1996).
[53] G. Karlström, R. Lindh, P.-Å. Malmqvist, B. O. Roos, U. Ryde, V. Veryazov, P.-O. Widmark, M. Cossi, B. Schimmelpfennig, P. Neogrady, and L. Seijo, Comput. Mater. Sci. **28**, 222 (2003).
[54] C. de Graaf, R. Broer, and W. C. Nieuwpoort, Chem. Phys. **208**, 35 (1996).
[55] C. de Graaf and R. Broer, Phys. Rev. B **62**, 702 (2000).
[56] C. Sousa, C. de Graaf, F. Illas, M. T. Barriuso, J. A. Aramburu, and M. Moreno, Phys. Rev. B **62**, 13366 (2000).
[57] C. Sousa, C. de Graaf, and G. Pacchioni, J. Chem. Phys. **114**, 6259 (2001).
[58] L. Giordano, P. V. Sushko, G. Pacchioni, and A. L. Schluger, Phys. Rev. Lett. **99**, 136801 (2007).
[59] U. Martinez, L. Giordano, and G. Pacchioni, J. Phys. Chem. B **110**, 17015 (2006).
[60] D. J. Tozer, R. D. Amos, N. C. Handy, B. O. Roos, and L. Serrano-Andres, Mol. Phys. **97**, 859 (1999).
[61] S. Grimme and M. Parac, ChemPhysChem **3**, 292 (2003).
[62] A. Dreuw, J. L. Weisman, and M. Head-Gordon, J. Chem. Phys. **119**, 2943 (2003).
[63] A. Dreuw and M. Head-Gordon, J. Am. Chem. Soc. **126**, 4007 (2004).
[64] D. J. Tozer, J. Chem. Phys. **119**, 12697 (2003).
[65] N. T. Maitra and D. G. Tempel, J. Chem. Phys. **125**, 18411 (2006).
[66] Z. L. Cai, K. Sendt, and J. R. Reimers, J. Chem. Phys. **117**, 5543 (2002).
[67] D. Jacquemin, E. A. Perpete, G. E. Scuseria, I. Coifini, and C. Adamo, J. Chem. Theory Comput. **4**, 123 (2008).
[68] S. T. Bromley, I. D. P. R. Moreira, F. Illas, and J. C. Wojdel, Phys. Rev. B **73**, 134202 (2006).